한국기계가공학회지, 제18권, 제5호, pp.9～16(2019.05) ISSN 1598-6721(Print)
Journal of the Korean Society of Manufacturing Process Engineers, Vol. 18, No. 5, pp.9~16(2019.05) ISSN 2288-0771(Online)

https://doi.org/10.14775/ksmpe.2019.18.5.009

Study of Brittle Crack Propagation Welding for EH40 Steel Plate in Shipbuilding Steel

Kyung-Shin Choi*, Sang-Hoon Lee*, Won-Jee Chung**,#, Hui-Geon Hwang**, Seok-Han Hong***, Ji-Ung Hong***
*Lloyds Register, **Changwon National University, ***HYUNDAI SAMHO HEAVY INDUSTRIES CO.,LTD.

조선용 EH40 강판의 용접부 취성 균열전파정지에 관한 연구

최경신*, 이상훈*, 정원지**,#, 황희건**, 홍석한***, 홍지웅***
*로이드선급, **창원대학교, ***현대삼호중공업

(Received 11 February 2019; received in revised form 7 March 2019; accepted 28 March 2019)

ABSTRACT

Recent economic trends are worsening and becoming longer, and Korean shipbuilding is focused on high value added and high technology, especially for LNG carriers and large container ships. Both ship types increased in size in the 2010s but have requirements such as high strength, toughness at low temperatures and continuous weldability for preventing brittle fractures at service temperatures. In particular, as container ships become larger, the International Classification Society (IACS) has established a provision (IACS UR S33) that mandates the use of BCA (Brittle Crack Arrest)-certified vessels for large container vessels contracted after 2014 to ensure safety. Therefore, studies on BCA 47Y.P are currently being undertaken, but BCA 40Y.P has not been actively studied yet. We will test BCA 40Y.P to verify why it can be applied to a large container ship and measure fatigue cracking.

Key Words : Brittle Crack Arrest(BCA, 취성 균열 정지 인성), International Classification Society(IACS, 국제선급협회), Crack Tip Opening Displacement(CTOD, 균열선단 열림 변위), Fatigue Pre-Cracking(피로 균열), Reverse Bending Method(역굽힘법)

1. Introduction

In recent years, the number of container ships owner by shipping companies has decreased somewhat due to a sudden recession. However, with the current revitalization of the economy of the shipping market, ordering competition for mega container ships is increasing again. The enlargement of container ships is advantageous for ship owners in terms of transportation efficiency and strategic dimensions. Since a decade ago, with the application of ultra-thick plates to the upper deck and hatch coaming parts of ships following the enlargement of 10,000-TEU or larger container ships, many studies have been conducted on 355MPa-grade steel with a thickness of 70mm or more. Furthermore,

Corresponding Author : wjchung@chanwon.ac.kr
Tel: +82-55-213-3624, Fax: +82-55-263-5221

with the construction of 20,000-TEU or larger container ships with high-strength, ultra-thick plates, 460MPa-grade YP47 steel plate is also being researched actively. For large container ships, as the steel applied to ships is becoming thicker, when cracks occur in the main steel of the hull girder strength, they do not stop but continue to progress. To address this problem, the ClassNK added new related regulations in 2007, which stimulated research on the fracture safety of ultra-thick plates[1-3]. The research on crack arrest started in 1953 when Robertson suggested the concept of crack arrest temperature[4].

Due to the nature of container ships, they have sharp stem and stern for fast speed, which cause insufficient reserve buoyancy and significant exposure in the hogging state. As a result, they are subject to high tension on the deck top and the deck's large opening for cargo loading, which affects the torsion of the entire ship and forms a torsion box on the upper deck. Furthermore, the longitudinal members have become thicker to compensate for the insufficient hull girder strength. According to recent brittle crack-stopping characteristics from the viewpoint of crack arrest for ultra-thick plates, as the steel thickness becomes larger than a certain value, the brittle cracks in the weld zones progress to the base metal and stop. However, for ultra-thick plates, the brittle cracks that start from the weld zone do not stop after progressing to the base metal but continue to progress straight along the weld line, causing serious safety problems. Therefore, to promote safety, the International Association of Classification Societies has prepared a regulation that obligates the use of BCA (Brittle Crack Arrest)-certified steel for large container ships that have contracted since 2014 (IACS UR S33)[5].

To examine research trends related to BCA, an analysis of specimens collected from 65mm or thicker welded steels revealed that the existence of stiffener designed to prevent brittle crack propagation in the weld zone could not prevent brittle crack propagation through the entire specimen[6]. Recently, studies have been conducted to address the productivity degradation problem of welding by applying electro-gas (EGW) welding instead of flux-cored arc welding (FCAW), which is frequently used to secure the structural safety of the hull, considering the welding process as well as the effect of the thickness in the evaluation of fracture toughness.

Several classification societies have found that the propagation path of brittle cracks that cause unstable fractures in ultra-thick plates for ships is considerably affected by welding residual stress as well. The engineering methods of domestic shipbuilding mostly adopt straight block butt joints instead of the cascaded type, which makes it more difficult to arrest brittle cracks. Consequently, the arrest of brittle crack propagation has been designed using arrest holes, arrest welding, and arrest inserts, and it has been reported that unstable fractures from the arrest of brittle crack propagation can be prevented based on research on special designs[7]. Ahn et al. conducted a study to achieve safety against unstable fractures by inducing cracks in BCA steel with excellent brittle crack arrest capacity regardless of the welding process when brittle cracks occur in the top structure of mega container ships[8].

In this study, a crack-tip opening displacement (CTOD) test was performed, which is a brittle fracture test, in addition to the conventional ESSO test for a 15,100-TEU large container ship that is under construction. In addition, a welding process that combines SAW with FCAW, which has been pointed out as a cause of welding productivity degradation, was applied to improve the low-impact strength after thermal treatment and prevent fractures due to the propagation of brittle cracks, thus achieving the safety of the welded structure.

2. Application of EH40 Certified Steel and Experimental Method

2.1 Application of steel

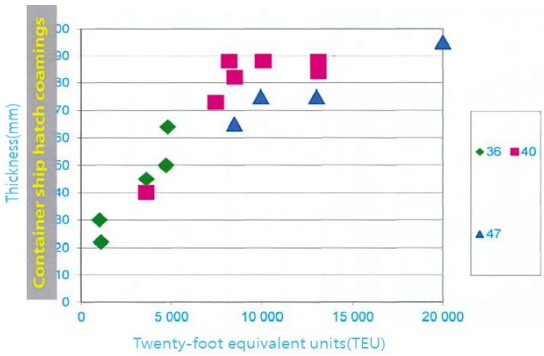

Fig. 1 Growth in containership size

For the steels in this study, YP40 Steel Plate, which is an ultra-thick steel for ships, and 80-mm-thick TMCP (Thermo Mechanical Control Process) of 390 MPa class, which is a high-quality high-strength steel for ships and offshore structures, were used. They were used at locations where deformations are caused due to major torsional stress in the upper deck and hatch coaming part of the 0.4-L section of the ship. Tables 1 and 2 show the chemical composition and mechanical characteristics of the certified steel.

Fig. 1 graphically shows application cases by size and thickness of large container ships. As shown in this graph, application cases are very rare for 15,000-TEU or larger ships. For mega container ships, the rule requirement of the classification societies has been satisfied using YP47, but this greatly increased the weight and cost of the ship due to over-scantling in some cases.

Table 1 Chemical composition of EH40 steel of used

Steels		C	Si	Mn	P	S	S-Al	Ceq	Pcm
YP 390	80 mm	0.06	0.13	1.68	0.0013	0.0013	0.003	0.43	0.18

Ceq=C+Mn/6+(Ni+Cu)/15+(Cr+Mo+V)/5
Pcm(%)=C+Si/30+Mn/20+Cu/20+Ni/60+Cr/20+Mo/15+V/10+5B

Table 2 Mechanical properties of base meter for EH40 steel of used

Steels		Yield Stress (MPa)	Tensile Strength (MPa)	Elongation (%)
YP390	80mm	507	598	24

With the progress of research on eco-friendly ships, an optimized design is being pursued by reducing the weight and fuel of the ships. In particular, the evaluation of YP40 is urgently needed, to which the classification rule for the evaluation of brittle crack arrest characteristics has not been applied.

2.2 Application of welding process and evaluation of unstable fracture safety

This study developed a welding process that can achieve the structural safety of ships against unstable fractures of ultra-thick steel plates. The developed method can arrest brittle cracks by combining FCAW and submerged arc welding (SAW) when cracks are propagated from the weld zone along the weld line while solving the productivity degradation problem of welding, which is a disadvantage of conventional FCAW. Fig. 2 shows the welding process, which combines FCAW and SAW.

Furthermore, in addition to the ESSO test, which has been generally used in brittle fracture toughness tests, the CTOD test was performed, which can measure the behaviors of the displacement of the crack surface, which is perpendicular to the original crack plane at the crack tip. Even if the weld zone of ultra-thick plates has passed nondestructive tests, such as radiographic, magnetic, and penetrant tests, they still have ultrafine weld defects, and the behaviors of structures when these defects are subjected to a load for a certain time can also be

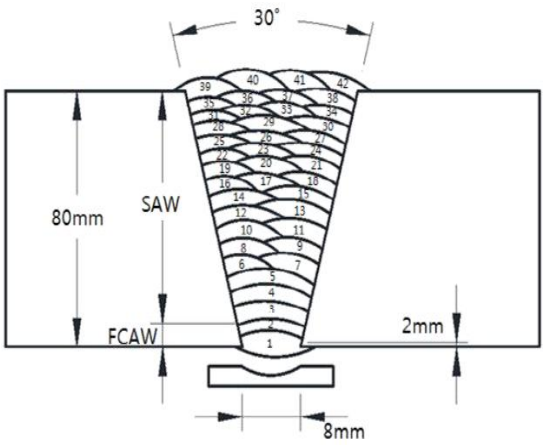

Fig. 2 Welding sequence of FCAW+SAW

Table 3 Test condition and mechanical properties

Specimen No	77t-SAW-1	77t-SAW-2	77t-SAW-3
Temp ℃		-10 ℃	
Standard		BS 7448-2 :1997	
Groove		1/2 Single V-Groove	
Notch position		HAZ	
TK(B)	76.87mm	76.87mm	76.86mm
Width(W)	76.82mm	76.84mm	76.83mm
Notch length		33 mm	
Spen		308 mm	
$Y(ao/W)$	2.753	2.781	2.721
Y S		557 MPa	
T S		623 MPa	

examined. The test conditions and mechanical properties of the test in the CTOD test are outlined in Table 3. Three specimens were fabricated to apply different conditions for the ratio of the mathematical function Y to verify the reproducibility in each test.

2.3 Reverse bending test

The general standards for the CTOD test are British Standard 7448 Part 1: 1991 and Part 2: 1997. Part 2 presents three test methods for preliminary fatigue crack morphologies: local compression, reverse bending, and stepwise high-R ratio. They give the maximum deviation allowance within 20% of the average value for preliminary fatigue crack morphologies. For residual stress deformations, local compression has been frequently used until recently as it is considered efficient for improving the preliminary crack morphologies of the weld zone. However, it is difficult to apply due to a rapid increase in the load resulting from the increased strength and thickness of materials[11].

The reverse bending method of BS 7448 Part 2: 1997 applies a bending load to the entire specimen through bending work after quenching the specimen and induces local plastic deformation at the notch tip. Thus, the load size is small and the procedure is simple. The coefficient of reverse bending stress intensity is determined with Eq. (1) using the maximum bending load by generating plastic deformation and a certain tensile residual stress at the notch root. In this equation, L denotes the notch constraint of a general rectangular specimen and ωrb denotes the plastic deformation area size as a result of reverse bending.

$$Krb = LR p0.2 \sqrt{\frac{8\omega rb}{\pi}} \quad (1)$$

When the size of the applied load is determined by calculating the coefficient of reverse stress intensity, the material toughness measured by the stress intensity factor must not exceed a certain value. Furthermore, the properties related to the fracture toughness must be determined experimentally. Thus, it is difficult to apply the reference load before the test. Therefore, the load at the time when macroscopic specimen damage occurs was defined as the reference load and the applied load was determined by applying the ratio derived from it.

3. Results and Discussion

3.1 Fatigue pre-cracking length and original crack length

The fatigue pre-cracking length was determined by measuring the actual fatigue crack length of one specimen in accordance with BS 7448 Part 1: 1991. It was derived from Eq. (2), and the actual crack length a_0 was determined by adding the fatigue crack length and the machined notch length, as shown in Eq. (3).

$$a_f = \frac{(a_{f0}+a_{f8})*0.5+a_{f1}+a_{f2}+a_{f3}+a_{f4}+a_{f5}+a_{f6}+a_{f7}}{8} \quad (2)$$

$$a_0 = M + a_f \quad (3)$$

As shown in Fig. 3, the measurements must be performed at nine points with equal intervals positioned at 1% of the thickness from the surface between the two external points, a_{f0} and a_{f8}. For the seven points excluding these two points, that is, between a_{f1} and a_{f7}, the points with equal intervals must be positioned on the inside of the surface.

Furthermore, the 0.2% resistance temperature for the fracture test can be calculated by the following Eq. (4):

$$\sigma_Y = \sigma_{Y0} + \frac{10^5}{(491+1.8*T)} - 189 \quad (4)$$

where T is the experimental temperature, $\sigma_{Y0}$is the fatigue crack temperature, and σ_Y is the fracture test temperature. All these temperatures mean 0.2% resistance temperatures.

Table 4 shows the fatigue pre-cracking results of the three specimens. The frequency is 10 times per second, that is, 10 Hz; the applied load in the final step of the fatigue crack extension is 5 kN, which is the maximum applied load for appropriate plastic deformation within a range that does not damage the material features; and the stress ratio is 10:1. Furthermore, the three specimens showed similar values for the maximum fatigue stress intensity factor applied in the fatigue crack stress step. The above-mentioned strength factor appeared in between 29,000 and 30,800 cycles on average. The ratios of the strength factor to the modulus of elasticity were also similar among the three specimens.

The average of the actual crack length was divided by the average of the length, and the differences between the maximum and minimum crack lengths are shown in Table 5. As shown in Figs. 4 and 5, none of the specimens had differences; thus, it can be seen that the reproducibility of the experiment was satisfied.

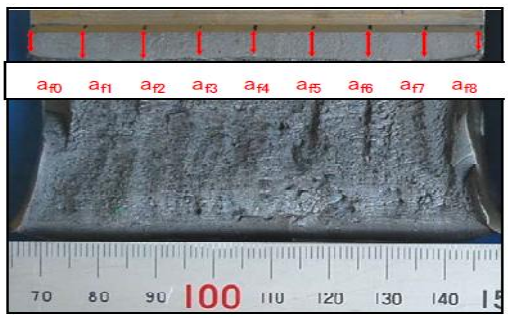

Fig. 3 Location of measurement point for specimen

Table 4 Test results of fatigue pre-cracking parameters

Specimen No	77t-SAW-1	77t-SAW-2	77t-SAW-3
Maximum fatigue precreckung force(F_f)		75 kN	
Stress ration(R)		0.1	
Maximum fatigue stress intensity factor(K_f)	39	39	38
Cycle number(Cycles)	30680	32065	29780
$\triangle K/E(m^{1/2})$	0.000170	0.000171	0.000168
Stress intensity factor(K)	153	146	144

Table 5 Test results of original crack length

Specimen No		77t-SAW-1	77t-SAW-2	77t-SAW-3
Original crack length (mm)	a_1	38.2	38.7	37.9
	a_2	40.0	40.0	39.6
	a_3	39.9	39.0	39.5
	a_4	39.6	39.1	39.3
	a_5	39.1	39.3	38.7
	a_6	38.7	39.7	38.5
	a_7	38.7	39.9	38.6
	a_8	39.2	40.1	39.3
	a_9	38.9	38.5	38.4
	a_0	39.2	39.5	38.9
	a_0 / W	0.510	0.514	0.507
Difference of each crack		0.047	0.040	0.044

Fig. 4 Fracture surface of 77t-SAW-1

Fig. 5 Fracture surface of 77t-SAW-2

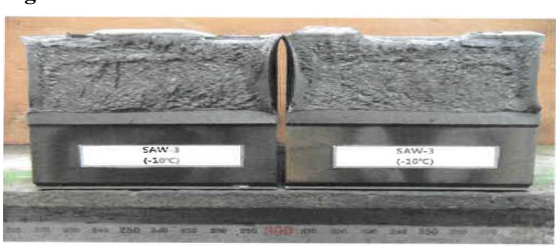

Fig. 6 Fracture surface of 77t-SAW-3

3.2 Crack tip opening displacement test

To cool down the specimens, they were placed in a mixture of liquid nitrogen, alcohol, and ice, and the experiment was performed after 40 min at the temperature of -10 ± 2℃. The temperature holding time was 30 s/mm, which was measured at around 2mm below the crack tips on both sides of the specimen. Fig. 5 shows the measuring instrument and tester used. The three-point bending test used the 1MN universal testing machine. The force and opening displacement were measured with voltage- and strain-measuring instruments. The experiment setup and measuring instruments are shown in Fig. 7.

BS 7448: Part 1: 1991 shows a correlation graph between the force and notch opening displacement. The calculation formula for the bending specimen is shown in Eq. (5).

$$K_Q = \frac{F_Q S}{B W^{1.5}} * f\left[\frac{a_0}{W}\right] \quad (5)$$

The above equation can be converted to Eq. (6) using the stress intensity factor (K_C) and the correct factor $(Y(\xi))$.

$$\delta_c = \frac{{K_C}^2 * (1-\upsilon^2)}{2\sigma_Y E} + \frac{0.4(W-a_0) * V_p}{0.4(W-a_0)+a_0+Z} \quad (6)$$

The stress intensity factor (K_C) can be calculated by Eq. (7) using the maximum force $p_{\max}$, strain coefficient $(Y(\xi))$, span, thickness, and width, and the correction factor can be expressed as Eq. (8):

$$K_C = \frac{P_{\max} * S * Y(\xi)}{B * W^{1.5}} \quad (7)$$

$$(Y_\xi) = \frac{3\xi^{0.5}[1.99-\xi(1-\xi)(2.15-3.98\xi+2.7\xi^2)]}{2(1+2\xi)(1-\xi)^{1.5}} \quad (8)$$

where δ_c is the CTOD (mm), E=Young's modulus is 206 GPa, υ is Poisson's ratio (0.3), a_0 is the

original crack length (mm), the span is 4 W(mm), Z is the knife edge thickness (mm), and , $Y(\xi)$ is the correction factor (N).

Figs. 8–10 show the graphs for the correlation between the clip gauge opening displacement and force.

The initial elastic zone is directly set by a person. In the graph, the y axis represents the force (kN) and the x axis represents the clip gauge opening displacement (mm), which means the (V_P) of the notch opening elasticity. As shown in 77-SAW-1, the line that starts from the (0, 0) point is an elastic section. The gauge opening displacement section (V_P) is 3.41 mm when the maximum load is 294.4 kN, and the opening displacement is 1.03 mm. This means that the material has more of its innate characteristic than the maximum 0.015 in the CTOD acceptance value required by API-PR 2Z.

Table 6 outlines the opening displacement results of the three specimens.

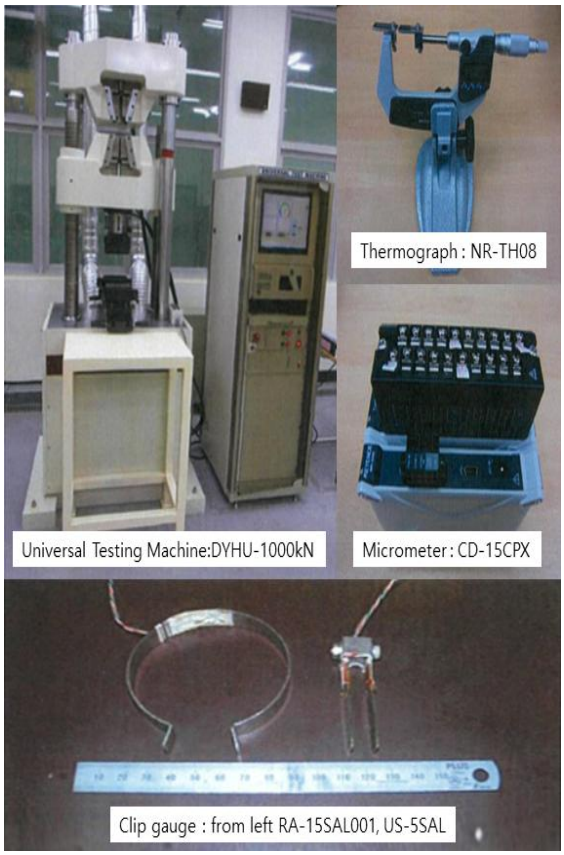

Fig. 7 Testing machine and measuring Instrument for CTOD test

Table 6 Test results of CTOD

Specimen	(V_P) mm	Max force (kN)	CTOD (mm)
77t-SAW-1	3.41	294.4	1.034
77t-SAW-2	1.14	278.2	0.394
77t-SAW-3	0.90	280.5	0.331

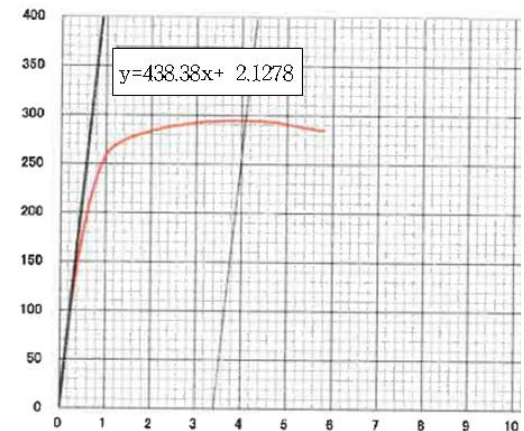

Fig. 8 Force and clip gauge opening of 77t-SAW-1

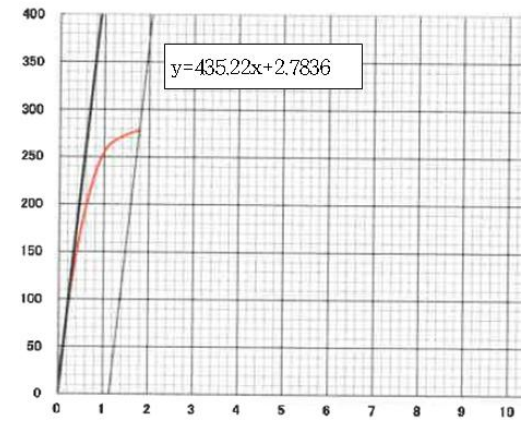

Fig. 9 Force and clip gauge opening of 77t-SAW-2

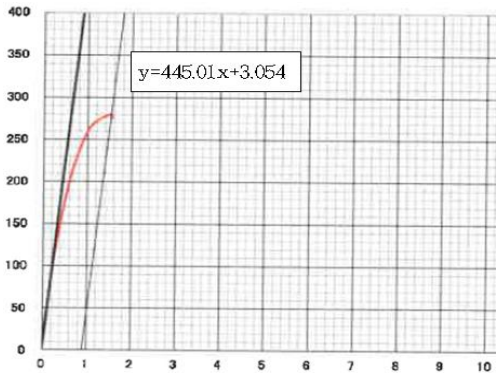

Fig. 10 Force and clip gauge opening of 77t-SAW-3

4. Conclusion

This study applied a welding process combining FCAW and SAW and satisfies the classification rules of EH40 BCA (Brittle Crack Arrest) steel for large container ships. The experiment results confirm the improved productivity of welding that can arrest the propagation of brittle cracks and ensure the hull structural safety of large container ships against brittle fatigue fractures.

REFERENCES

1. Handa, T., Suzuki, S., Tokura, M., Kiji, N., Nakanishi, Y., "Behavior of long brittle crack arrest in Tee joint structure of thick plate," Bulletin of the Japan Society of Naval Architects and Ocean Engineering, Vol. 4, pp. 461-462, 2007.
2. Honda, T., Kubo, T., Kawabata, F., Nishimura, K., Suzuki, S., Shiomi, H., Miyata, T., "Effect of Kca value on behavior of brittle crack arrest in Tee joint structure of thick plate," Bulletin of the Japan Society of Naval Architects and Ocean Engineering, Vo1. 4, pp. 459-460, 2007.
3. Inoue, T., Ishikawa, T., Imai, s., Koseki, T., Hirota, K., Yamaguchi, Y., Matsumoto, Y., Yajuma, H., "Long crack arrest concept in heavy-thick shipbuilding steels," Pro-ceedings of International Offshore and Polar Engineering Conference, pp. 3322, 2007.
4. Robertson, T. S., "Propagation of brittle fracture in steel," Journal of the Iron and Steel Institute, Vol. 175, pp. 361-374, 1953.
5. Yamaguchi, Y., Yajima, H., Aihara, S., Yoshinari, H., Hirota, K., Toyoda, M., Kiyosue, T., Tanaka, S., Okabe, S., Kageyama, K., Funatsu, Y., Handa, T., Kawabata, T., Tani, T., "Development of guidelines on brittle crack arrest design-Brittle crack arrest design for large container ships-1," International Society of Offshore and Polar Engineers, pp. 20-25, 2010.
6. Inoue, T., Ishikawa, T., Imai, S., koseki, T., Hirota, K., Tada, M., Kitada, H., Yamaguchi, Y., Yajima, H., "Long crack arrestability of heavy-thick shipbuilding steels," International Society of Offshore and Polar Engineers, Vol. 16, 2006.
7. An, G. B., “Unstable Fracture Preventive Design in Large Vessels and Offshore Structures,” International Journal of Offshore and Polar Engineering, Vol. 25, No. 3, 2015.
8. An, G. B., Han, I. W., Park, J. U., Woo, W. C., "A Basic Study on Brittle Crack Propagation Path with Ultra Large Steel Plate Weld Joints," Journal of Welding and Joining, Vol. 35, No. 6, pp. 15-20, 2017.
9. Jeong, S. H., Park, D. H., Kim, H. S., Shin, S. B., Park, T. J., "A Study on Reduction of Pre-Crack Deviation in CTOD Specimen Using Reverse Bending Method", Journal of Welding and Joining, Vol. 33 No. 2, pp. 62-68, 2015.
10. James, G., William, T., Yong-Yi Wang, Y. Y., Bowker, J., Park, D. Y., Guowu, S., "Mechanical properties and microstructure of weld metal and HAZ regions in X100 single and dual torch girth welds," 2010 8th International Pipeline Conference, Vol. 2, pp. 619-629, 2010.